Enhanced Photocurrent in Al/Porphyrin Schottky Barrier Cell with Heterodimer Consisting of Metal-Free Porphyrin and Zinc Porphyrin

Kohshin Takahashi,* Tadashi Goda, Takahiro Yamaguchi, and Teruhisa Komura

Department of Chemistry and Chemical Engineering, Faculty of Engineering, Kanazawa University, Kodatsuno, Kanazawa 920-8667, Japan

Kazuhiko Murata*

R & D Promotion Department, Nippon Shokubai Co., Ltd., Nishi-Otabi, Suita 564-8512, Japan

Received: December 10, 1998; In Final Form: February 22, 1999

An Al/porphyrin Schottky barrier cell with an equimolar mixed solid of a weak electron-donating zinc porphyrin such as 5,10,15,20-tetra(2,5-dimethoxyphenyl)porphyrinatozinc (Zntpp$(OMe)_2$) and a weak electron-accepting metal-free porphyrin such as 5,10,15-triphenyl-20-(3-pyridyl)porphyrin (H_2pyp_3p) shows much larger photocurrent compared to the cells with the pure Zntpp$(OMe)_2$ solid and with the pure H_2pyp_3p solid. Relatively large values, short-circuit photocurrent quantum yield of 18.9%, open-circuit photovoltage of 0.79 V, fill factor of 0.23, and energy conversion yield of 1.21% are obtained for the cell with the mixed solid when illuminated by a monochromatic light of 445 nm with light intensity of 7 μW cm^{-2}. The series resistance of the mixed solid cell is as large as that of the pure Zntpp$(OMe)_2$ cell; the potential gradient in the depletion layer near the Al/mixed solid interface is smaller than that near the Al/pure Zntpp$(OMe)_2$ solid interface; and the exciton diffusion lengths in the pure Zntpp$(OMe)_2$ solid, the pure H_2pyp_3p solid, and the mixed solid are almost the same. Thus, the photocurrent enhancement for the mixed solid is not explained by these factors. The enhancement is interpreted by the ease of a photoinduced intramolecular electron transfer of a porphyrin heterodimer produced by an axial coordination of pyridyl group in H_2pyp_3p to zinc ion in Zntpp$(OMe)_2$ in the mixed solid because the charge-separated dimer can separate to a free electron and a free hole under a large electric field formed near the Al/porphyrin interface much more easily than the excited pure porphyrins.

Introduction

Organic solar cells have been expected as low-cost solar cells for past two decades. We can classify roughly a number of studies about them[1−44] according to two types of approaches that have been taken for designing such cells. One is the physical approach based on the theory for semiconductors.[1−26] The most successful example was the organic p−n junction cells consisting of a copper phthalocyanine and a peryrene tetracaboxylic derivative with a relatively large power conversion efficiency (1%) by Tang.[19] However, the efficiency is not satisfactory for practical use because of the high resistance and low mobility of the organic layers compared to those in inorganic cells. Therefore, exceeding the efficiency of inorganic cells seems to be difficult because of the inferior physical properties as semiconductors and as far as relying on the theory for semiconductors that is developed for inorganic semiconductors.

The other and more promising approach for organic solar cells is designing the sophisticated charge-separation system.[27−32] Many porphyrin derivatives linked covalently by an electron acceptor and/or a donor have been synthesized, and the kinetics of their photoinduced electron transfer in solution has been investigated by photophysical methods such as transient spectroscopy.[45−58] For an efficient conversion of solar energy to electric and/or chemical energy, it is important to prolong the lifetime of charge-transfer-states formed from the excited reaction center by suppressing charge recombination. For example, Osuka et al.[59] and Sauvage et al.[60] recently reviewed that the photocharge transfer states of multicomponent porphyrin compounds well-arranged energetically by a covalent or coordinate bond had considerably long lifetimes (longest lifetime in the reviews is 16 μs) because the photoproduced electron and hole can separate from each other at large distances, suppressing back-electron-transfer. Imahori et al.[61,62] also recently reported that photoinduced electron transfer in covalently linked porphyrin−fullerene compounds was accelerated and that their charge recombination was fairly retarded compared to that in covalently linked porphyrin-acceptor compounds, which have low-molecular-weight acceptors because large conjugating systems of fullerenes can delocalize charges. Further, Fox et al.[63,64] showed that depending on the order for arranging the *N*,*N*-dimethylaniline as a donor and pyrene as an acceptor along the dipole of attaching dichromophoric α-helical peptides, the photoinduced intramolecular electron transfer was accelerated or slowed. Thus, we believe that an efficient photoenergy conversion can be attained by using a well-designed molecular system such as that described above.

We have taken the following strategy to obtain a fundamental perspective for preparing efficient solar cells. First, we used the mixed dye complexes consisting of an electron-donor dye and an electron-acceptor dye, which can be prepared by mixing the dyes in solution. Second, the dye complexes were placed in a high built-in potential simply accomplished by spin-coating the complexes onto the Al substrate. Because the dyes with high electric resistance hardly create a semiconducting band, they

10.1021/jp984706f CCC: $18.00
Published on Web 05/20/1999

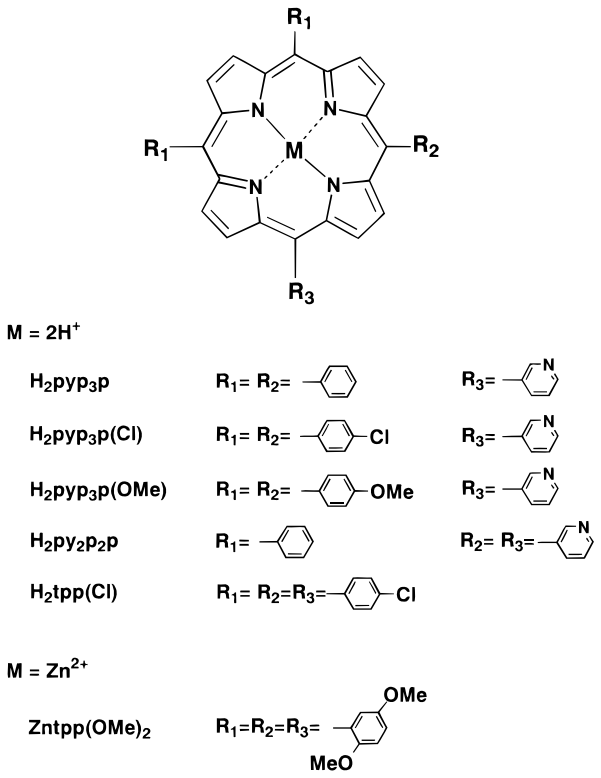

Figure 1. Structures and abbreviations of porphyrins.

can be regarded as both photosensitizer and multistage array of donors and acceptors. We reported that enhanced photocurrent was observed for the Al/dye Schottky barrier cells using the molecular complex of zinc porphyrin and rhodamine B[37] and using the complex of zinc porphyrin and merocyanine.[36,38] We also reported in a preliminary result[35] of this study that we can prepare a spin-coated solid film of heterodimer consisting of a zinc porphyrin donor such as 5,10,15,20-tetra(2,5-dimethoxyphenyl)porphyrinatozinc, Zntpp(OMe)$_2$, and a metal-free porphyrin acceptor such as 5,10,15-triphenyl-20-(3-pyridyl)-porphyrin, H$_2$pyp$_3$p, where pyridyl group in H$_2$pyp$_3$p coordinates to the central Zn ion in Zntpp(OMe)$_2$ by mixing in a noncoordinating solvent such as chloroform, and the Al/heterodimer Schottky barrier cell exhibited a much larger photocurrent than the cell with pure Zntpp(OMe)$_2$ or pure H$_2$pyp$_3$p. In the present paper, we show in detail why the enhanced photocurrent was observed for the cell with heterodimers consisting of Zntpp-(OMe)$_2$ and various metal-free porphyrin derivatives with different redox potentials.

Experimental Section

Porphyrin compounds as shown in Figure 1 were synthesized by literature methods and purified by column chromatography on alumina and silica gel.[65−67]

Sandwich-type photocells of Al/dye/Au were fabricated as in a previous paper.[37] It should be noted that the actual cell structure is Al/Al$_2$O$_3$/dye/Au because Al in air is oxidized quickly to form a layer of Al$_2$O$_3$. The dye films were prepared on the aluminum-coated glass substrate with the transmittance at 500 nm of 10 ± 2% (Al thickness was 22 ± 3 nm) by spin-coating. The thickness of the spin-coated dye films was estimated from the amount and the density of dye on the substrate. The amount was determined by a Hitachi U-3210 UV−visible spectrometer after dissolving the layer into chloroform. The mixing ratio in the mixed dye solid was regarded as the same as that in the spin-coated chloroform solution. The value of 1.3 g cm^{-3}, determined pycnometrically with water/ethanol (3:7 by weight) for a solid of 5,10,15,20-tetraphenylporphyrinatozinc, was assumed as the density of pure porphyrin solids and mixed solids.

The photocurrent and photovoltage measurements were made as in a previous paper.[37] All electrical measurements were performed in air at a temperature of 22 ± 3 °C and a relative humidity of 40 ± 10% after the prepared cell stood for 1 day at room temperature in a dark desiccator controlled with a relative humidity of 45% by concentrated sulfuric acid to obtain a steady photocurrent. Since the photocurrent of an Al/metal-free tetrabenzporphyrin Schottky barrier cell gradually decreased with time, as we have shown in ref 26, those of Al/porphyrin Schottky barrier cells used here were measured immediately after irradiation. Further, cyclic voltammetry was also performed as in a previous paper.[37] The half-wave potential, or the redox potential, measured at a scan rate of 100 mV s^{-1} was the average of the cathodic and anodic peak potentials and was described on the basis of the half-wave potential of ferrocenium ion/ferrocene(Fc$^+$/Fc).

Results

Enhanced Photocurrent of Al/Porphyrin Schottky Barrier Cells with Equimolar Mixed Solid of H$_2$pyp$_3$p and Zntpp-(OMe)$_2$. Parts a and b of Figure 2 show the short-circuit photocurrent action spectra of Al/dye/Au sandwich-type cells with pure H$_2$pyp$_3$p solid and with pure Zntpp(OMe)$_2$ solid, respectively, accompanied by the absorption spectra of the solid films on a slide glass. The photocurrent flows from the Au electrode to the Al electrode through the external circuit for irradiation from both sides. The action spectra follow the absorption spectra only when the cells are illuminated from the Al side, but the smaller photocurrents due to the absorption by the porphyrin layer, the so-called optical filter effect, are observed at the Soret band when illuminated from the Au side. These indicate that the photocurrent originates from the charge separation of the excited singlet state of porphyrins at the potential gradient in the porphyrin solids near the Al/dye interface. Such a potential is produced by the contact of a low-work-functional Al and a porphyrin solid with large resistance (ca. 10^{11}−10^{13}Ω cm^{-1}) such as H$_2$pyp$_3$p and Zntpp(OMe)$_2$ in which the dark-conducting carriers are holes.[9−13]

Parts a and b of Figure 3 show current−voltage curves for Al/H$_2$pyp$_3$p/Au and Al/Zntpp(OMe)$_2$/Au cells, respectively. The short-circuit dark current is zero for the both cells, and when a potential of more than 1 V is applied to the Au electrode with respect to the Al electrode, namely, with application of a forward bias of more than 1 V, a large dark current flows from the Al electrode to the Au electrode through the external circuit though the current of the Al/H$_2$pyp$_3$p/Au cell is smaller than that of the Al/Zntpp(OMe)$_2$/Au cell. The series resistance of the cells with 0.25 cm^2 active area, estimated roughly from the slope of the $J-V$ curves in the range of the forward bias, is 3.3 × 10^8 Ω for Al/H$_2$pyp$_3$p (d = 15 nm)/Au and 1.3 × 10^6 Ω for Al/Zntpp(OMe)$_2$ (d = 17 nm)/Au, indicating that the latter resistance is 2 orders of magnitude smaller than the former resistance, where d represents the film thickness. The solid consisting of Zntpp(OMe)$_2$ molecules with a lower ionization threshold energy has a larger hole density than the solid consisting of H$_2$pyp$_3$p molecules because the former oxidation by the oxygen molecules physisorbed in the solid is easier than the latter oxidation. The oxidation potential in dichloromethane is 0.30 V vs Fc$^+$/Fc for Zntpp(OMe)$_2$ and 0.58 V for H$_2$pyp$_3$p.

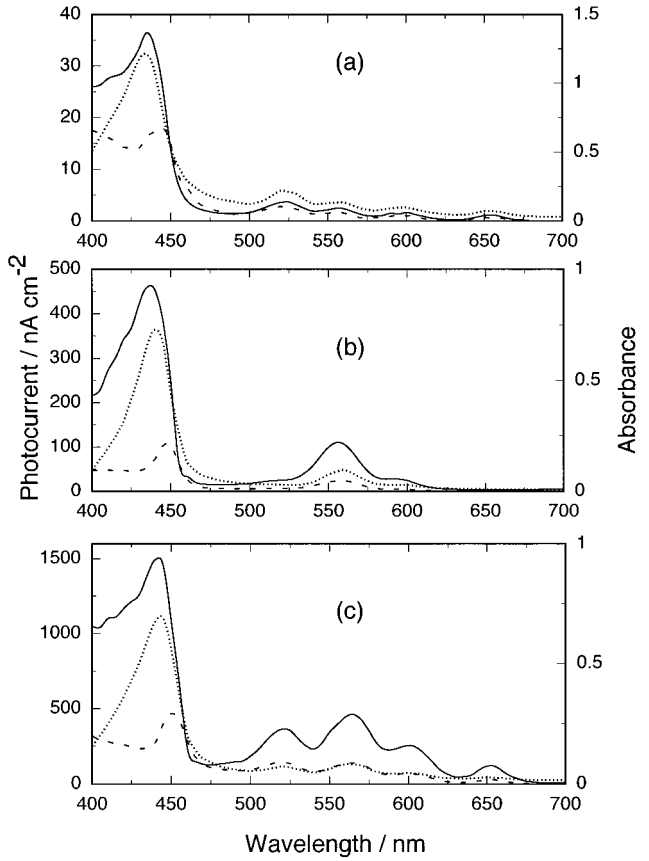

Figure 2. Photocurrent action spectra of Al/H_2pyp_3p (d = 45 nm)/Au (a), Al/Zntpp(OMe)$_2$ (d = 45 nm)/Au (b), and Al/Zntpp(OMe)$_2$−H_2-pyp_3p (R = 0.5, d = 45 nm)/Au (c) cells, where d and R indicate the thickness of porphyrin solid film and the molar ratio of metal-free porphyrin to total porphyrin, respectively. The light intensities at the Al/porphyrin and the Au/porphyrin interfaces were normalized to 20 μW cm^{-2}. The solid line represents the irradiation from the Al side, the broken line represents the irradiation from the Au side, and the dotted line represents the absorption spectra of the porphyrin solid films (d = 20 nm) on a slide glass.

Thus, the Zntpp(OMe)$_2$ solid has smaller resistance than the H_2pyp_3p solid, and eventually, the series resistance of the Al/Zntpp(OMe)$_2$/Au cell is smaller than that of the Al/H_2pyp_3p/Au cell. An unsaturated photocurrent flowing from the Au electrode to the Al electrode through the external circuit is observed for both cells with application of the reverse bias because of a space-charge limitation in the large resistance of the Zntpp(OMe)$_2$ and H_2pyp_3p solids. The photocurrent of the Zntpp(OMe)$_2$ cell is larger than that of the H_2pyp_3p cell because the series resistance of the former cell is much smaller than that of the latter cell.

Figure 2c shows the short-circuit photocurrent action spectra of an Al/heterodimer/Au cell with an equimolar mixed solid (R = 0.5) of Zntpp(OMe)$_2$ and H_2pyp_3p and the absorption spectrum of the mixed solid on a slide glass, where the mixing ratio R is defined as the molar ratio of metal-free porphyrin to total porphyrin. Fleisher and Shachter[65] showed that the pyridyl group in 5,10,15-triphenyl-20-(4-pyridyl)porphyrin coordinated to the central zinc ion in 5,10,15,20-tetraphenylporphyrinatozinc in chloroform, and further, a linear polymer was formed by such a coordinate bond in a solid consisting of 5,10,15-triphenyl-20-(4-pyridyl)porphyrinatozinc. This means that the number of coordination for the central Zn ion is five. If the number is more than six, a branched or cross-linked polymer would be obtained. Therefore, a heterodimer can be formed in the mixed solid of Zntpp(OMe)$_2$ and H_2pyp_3p because of such an axial coordination. This is supported from the evidence that the Soret peak in the mixed solid shifts to longer wavelength compared to those in pure porphyrin solids in a similar manner as the Soret peak shift observed by the axial coordination of various ligands to zinc porphyrin in nonbonding solvents.[68] The photocurrent action spectrum obtained by irradiating from the Al side follows the absorption spectrum, and an optical filter effect of the photocurrent is observed when illuminated from the Au side. This indicates that the photoactive side is the Al/dye interface because dark-conducting carriers in the mixed solid are holes in analogy with the pure porphyrins, and eventually, a potential gradient builds up in the mixed solid near the Al/dye interface. The remarkable characteristics for the mixed porphyrin cell are that the photocurrent is about 40 times larger than that of the pure H_2pyp_3p cell and is about 3 times larger than that of the pure Zntpp(OMe)$_2$ cell.

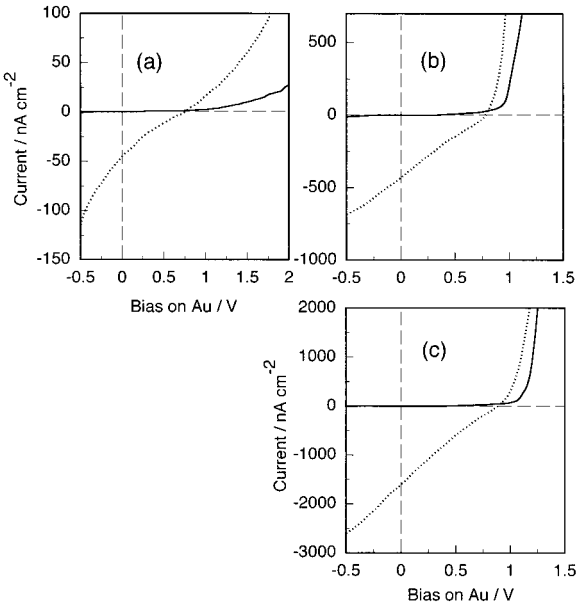

Figure 3. Dark current−voltage (solid line) and photocurrent−voltage (dotted line) characteristics by irradiating from the Al side at the Soret peak wavelength for Al/H_2pyp_3p (d = 15 nm)/Au (a), Al/Zntpp(OMe)$_2$ (d = 17 nm)/Au (b), and Al/Zntpp(OMe)$_2$−H_2pyp_3p (R = 0.5, d = 19 nm)/Au (c) cells. The light intensity at the Al/porphyrin interface was normalized to 20 μW cm^{-2}.

The current−voltage curves for the mixed solid cell are similar to the curves of the pure solid cells (see Figure 3). Short-circuit photocurrent quantum yield ϕ (%), open-circuit photovoltage V_{oc}, fill factor ff, and the energy conversion yield η (%) estimated from these J−V curves are summarized in Table 1. Since the ϕ value of the mixed solid cell is much larger than those of both cells with the pure solids, the enhanced η value is obtained for the mixed solid cell though the V_{oc} and ff values are not improved. In the Al/Zntpp(OMe)$_2$−H_2pyp_3p (R = 0.5, d = 19 nm)/Au cell, better values of ϕ = 18.9%, V_{oc} =0.79V, ff =0.23, and η =1.21% are obtained when monochromatic light of λ = 445 nm with I_0 = 7 μW cm^{-2} is illuminated from the Al side, where λ and I_0 are the wavelength of the incident light and the light intensity at metal/dye interface, respectively. Since the mixed solid cell has the same series resistance (1.3×10^6 Ω) as the pure Zntpp(OMe)$_2$ cell, the reason for the photocurrent enhancement is not due to the decrease of the solid resistance by mixing Zntpp(OMe)$_2$ and H_2pyp_3p. We will discuss later why the photocurrent is enhanced when the mixed solid film prepared by the simple spin-coating method is used for the Al/dye Schottky barrier cell.

TABLE 1: Performance of Al/Porphyrin Schottky Barrier Cells[a]

porphyrin	R[b]	d[c] (nm)	λ[d] (nm)	ϕ[e] (%)	V_{oc}[f] (V)	ff[g]	η[h] (%)
$H_2pyp_3p(OMe)$		22	440	0.84	0.94	0.26	0.042
H_2pyp_3p		15	440	0.49	0.75	0.20	0.027
$H_2pyp_3p(Cl)$		20	440	0.26	0.72	0.24	0.011
$Zntpp(OMe)_2$		17	440	6.1	0.78	0.23	0.38
$H_2pyp_3p(OMe)-Zntpp(OMe)_2$	0.50	23	445	12.9	0.79	0.22	0.81
$H_2pyp_3p-Zntpp(OMe)_2$	0.50	19	445	18.9	0.79	0.23	1.21
$H_2pyp_3p(Cl)-Zntpp(OMe)_2$	0.46	20	445	25.3	0.63	0.24	1.39
$H_2tpp(Cl)-Zntpp(OMe)_2$	0.55	21	440	17.0	0.91	0.21	1.17
$H_2py_2p_2p-Zntpp(OMe)_2$	0.48	19	445	22.5	0.89	0.21	1.50

[a] The light intensity transmitted through the Al electrode is about 8 ± 2 μW cm^{-2}. [b] Molar ratio of metal-free porphyrin to total porphyrin. [c] Film thickness. [d] Wavelength of incident light. [e] Short-circuit photocurrent quantum yield. [f] Open-circuit photovoltage. [g] Fill factor. [h] Energy conversion yield.

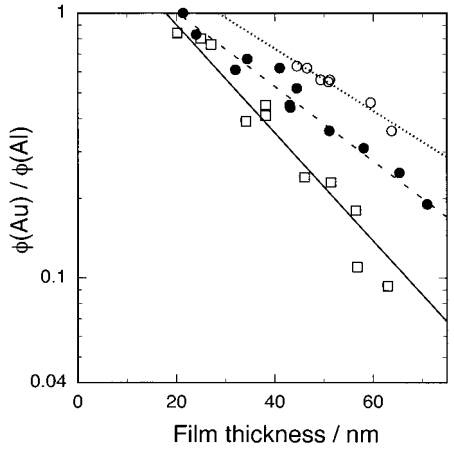

Figure 4. Plot of the value of ϕ(Au)/ϕ(Al) at the Soret peak wavelength as a function of the thickness of porphyrin film. Symbols are the experimental values, and lines are estimated by calculation: (○) H_2pyp_3p; (dotted line) $W_{ap} = 24$ nm, $L_{exc} = 12$ nm; (●) $Zntpp(OMe)_2-H_2pyp_3p$ ($R = 0.5$); (broken line) $W_{ap} = 16$ nm, $L_{exc} = 10$ nm; (□) $Zntpp(OMe)_2$; (solid line) $W_{ap} = 6$ nm, $L_{exc} = 10$ nm.

Estimation of the Width of Schottky Barrier Formed near the Al/Porphyrin Interface and the Exciton Diffusion Length in the Porphyrin Solid. The primary process for photocurrent generation in Al/porphyrin Schottky barrier cells is that excitons are formed in the Schottky barrier under illumination or excitons formed in the bulk solid migrate into the barrier, and then they separate to free charges of electrons and holes by an electric field present in the barrier. Thus, the photocurrent gets larger as the electric-field gets larger and the exciton diffusion length gets longer. That is, the two values are very important for clarifying the dominant factors of the magnitude of the photocurrent.

It is expected that the optical filter effect, a smaller photocurrent observed by irradiating from the side of the ohmic interface, becomes large as the depletion layer becomes narrow and the thickness of dye film becomes thick, because the dye layer prevents the approach of photons to the photoactive interface. This effect is the more important the smaller the diffusion length of the excitons is. The dye solid with higher carrier density should have a narrower depletion layer because of the more effective charge compensation for the blocking contact between the metal and dye solid. Figure 4 shows the dependence of the optical filter effect represented by ϕ(Au)/ϕ(Al) on the film thickness, where ϕ(Au) is the short-circuit photocurrent quantum yield at the Soret peak of porphyrin for the irradiation from the Au side and ϕ(Al) is that for the irradiation from the Al side.

The apparent width of the Schottky barrier W_{ap} and the exciton diffusion length L_{exc} are estimated by reproducing the plot in Figure 4 with an exciton dissociation model, proposed by Yamashita et al.,[69] being applied to Schottky type porphyrin organic solar cells. This model consists of the following theoretical proposals. The photogenerated charge carriers are attributable to the dissociation of excitons diffusing toward the Schottky barrier in the electric-field, and the quantum efficiency of carrier generation is not constant over the dye layer but exponential at the barrier, assuming exponential distribution of dopant O_2, which can be undoped by outgassing the dye solid under vacuum. Further, the W_{ap} is a distance where the electric field becomes 1/e of the maximum field at the metal/dye interface. The W_{ap} and the L_{exc} contained in the equations for describing the model are evaluated by numerical calculations using the Montes Carlo method with a computer.[37,38,69]

Figure 4 shows the calculated lines for the optical filter effects of the pure $Zntpp(OMe)_2$ cell, the pure H_2pyp_3p cell, and the equimolar mixed solid cell. Since the estimated lines by the proposed model approximately agree with the experimental plots as shown in Figure 4, the model seems reasonable. The values of $W_{ap} = 5 \pm 3$ nm and $L_{exc} = 10 \pm 6$ nm for $Zntpp(OMe)_2$, $W_{ap} = 16 \pm 4$ nm and $L_{exc} = 11 \pm 9$ nm for $Zntpp(OMe)_2-H_2pyp_3p$ ($R = 0.5$), and $W_{ap} = 24 \pm 6$ nm and $L_{exc} = 13 \pm 9$ nm for H_2pyp_3p are obtained. The W_{ap} of the $Zntpp(OMe)_2$ cell is considerably narrower than that of the H_2pyp_3p cell as predicted from the hole density in the pure solids, and the W_{ap} of the mixed solid cell exhibits their intermediate value.

Because the V_{oc} value approximately indicates the difference between both Fermi levels of the Al constituting the photoactive interface and the flat-band state of the dye solid, the potential step corresponding to the V_{oc} value exists in the Schottky barrier under the short-circuit condition. Thus, the potential gradient is estimated roughly from the ratio of the V_{oc}/e and W_{ap} values because the W_{ap} is the distance where the potential step V_{oc} becomes 1/e.[69] Since the V_{oc} values of the $Zntpp(OMe)_2$ cell, the H_2pyp_3p cell, and the mixed solid cell are almost the same (see Table 1), the potential gradient is governed by the W_{ap} value. That is, the gradient decreases in the order $Zntpp(OMe)_2$ > $Zntpp(OMe)_2-H_2pyp_3p$ > H_2pyp_3p, and the potential slope is on the order of 10^5 V cm^{-1}. Since this order of the potential slope does not agree with the order of magnitude of the photocurrent, i.e., $Zntpp(OMe)_2-H_2pyp_3p$ > $Zntpp(OMe)_2$ > H_2pyp_3p, and further the L_{exc} values are almost the same, the enhanced photocurrent for the mixed solid cell is not explained by these factors.

Enhanced Photocurrent of Al/Porphyrin Schottky Barrier Cells with Mixed Solids Consisting of a Weak Donating $Zntpp(OMe)_2$ and Various Weak Accepting Metal-Free Porphyrins. Figure 5 shows the dependence of the ϕ value at the Soret peak wavelength on the mixing ratio R of the mixed solids $Zntpp(OMe)_2-H_2pyp_3p(Cl)$, $Zntpp(OMe)_2-H_2pyp_3p$, and $Zntpp(OMe)_2-H_2pyp_3p(OMe)$, where R is the molar ratio of

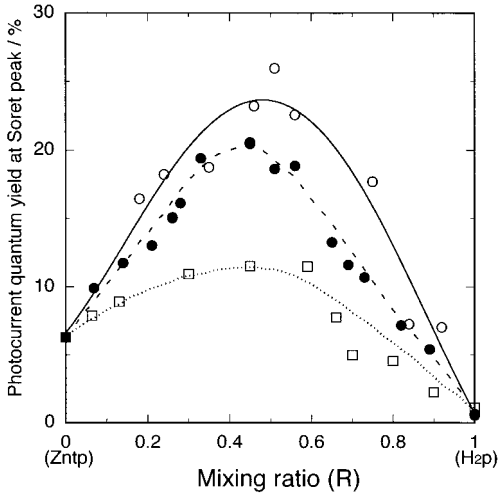

Figure 5. Relation between mixing ratio (R) and short-circuit photocurrent quantum yield at the Soret peak for Al/Zntpp(OMe)$_2$−H$_2$pyp$_3$p(Cl)/Au (○), Al/Zntpp(OMe)$_2$−H$_2$pyp$_3$p/Au (●), and Al/Zntpp(OMe)$_2$−H$_2$pyp$_3$p(OMe)/Au (□) cells. The film thickness of the porphyrin solids is about 20 nm, and the irradiation is done from the Al side by monochromatic light of the Soret peak wavelength with an intensity of about 8 ± 2 μW cm^{-2}.

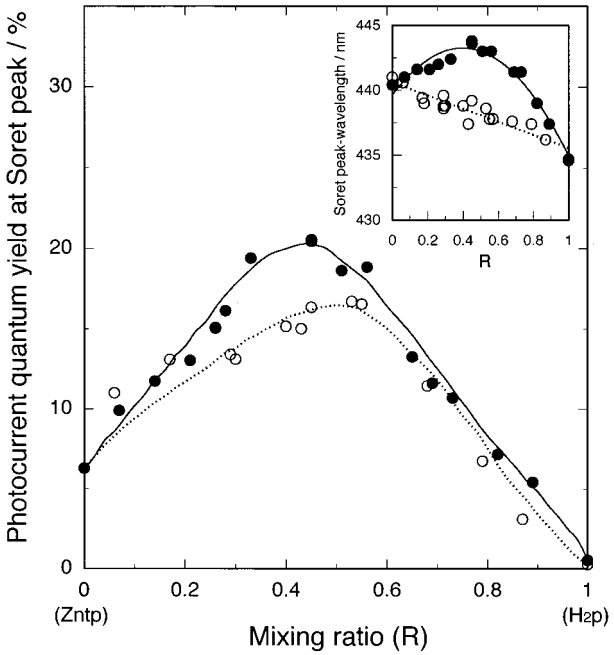

Figure 6. Relation between mixing ratio (R) and short-circuit photocurrent quantum yield at the Soret peak for Al/Zntpp(OMe)$_2$−H$_2$pyp$_3$p/Au (●) and Al/Zntpp(OMe)$_2$−H$_2$tpp(Cl)/Au (○) cells. The film thickness of the porphyrin solids is about 20 nm, and the irradiation is done from the Al side by monochromatic light of the Soret peak wavelength with an intensity of about 8 ± 2 μW cm^{-2}. The inset is the R dependence of the Soret peak wavelength for the porphyrin solid films of Zntpp(OMe)$_2$−H$_2$pyp$_3$p (●) and Zntpp(OMe)$_2$−H$_2$tpp(Cl) (○).

metal-free porphyrin to total porphyrin. It is found from the optical filter effect, as observed in the photocurrent action spectra, that the photoactive side is the Al/dye interface because dark-conducting carriers in the mixed solids and the pure porphyrin solids constituting these photocells are holes. The photocurrent exhibits a maximum around $R = 0.5$, suggesting that there is an interaction between Zntpp(OMe)$_2$ and metal-free porphyrin in the spin-coated mixed solid, and the interaction acts favorably for the photocharge separation. The ϕ value is in the order of Zntpp(OMe)$_2$−H$_2$pyp$_3$p(Cl) > Zntpp(OMe)$_2$−H$_2$pyp$_3$p > Zntpp(OMe)$_2$−H$_2$pyp$_3$p(OMe). Since the used metal-free porphyrins have a similar structure, heterodimers with a similar structure may be formed by the axial coordination of the pyridyl group in the metal-free porphyrins to the central zinc ion in Zntpp(OMe)$_2$. In the Zntpp(OMe)$_2$−H$_2$pyp$_3$p equimolar mixed solid, the fluorescence peaks at 612 and 658 nm for Zntpp(OMe)$_2$ are completely quenched under electric-field-free conditions (e.g., the films on glass substrates), and the intensity of the fluorescence peaks at 668 and 724 nm for H$_2$pyp$_3$p is somewhat increased compared to the intensity in pure H$_2$pyp$_3$p solid. Because most of the emission spectrum of Zntpp(OMe)$_2$ overlaps with the absorption spectrum of H$_2$pyp$_3$p, an energy-transfer of Förster type may occur from the excited Zntpp(OMe)$_2$ to the ground-state H$_2$pyp$_3$p in the porphyrin heterodimer. If the ground-state of H$_2$pyp$_3$p was occupied by the transferred electron from the excited Zntpp(OMe)$_2$, the fluorescence of H$_2$pyp$_3$p would decrease. Thus, the increase of the fluorescence intensity of H$_2$pyp$_3$p means that no electron transfer occurs in the absence of an electric field. Since the optical filter effect as observed in the photocurrent action spectra for the heterodimer photocell is reproduced by Yamashita's model as mentioned in a former section, it is inferred that excitons arising from the excited metal-free porphyrins in the porphyrin heterodimer arrive at the Schottky barrier. Then the excitons may dissociate to zinc porphyrin cations and metal-free porphyrin anions by an intramolecular electron transfer only under such a large electric field as the Schottky barrier. The thermodynamic driving force for the electron transfer from the Zntpp(OMe)$_2$ in the ground state to the excited singlet state of metal-free porphyrin is about 0.35 eV for Zntpp(OMe)$_2$−H$_2$pyp$_3$p(Cl), about 0.28 eV for Zntpp(OMe)$_2$−H$_2$pyp$_3$p, and about 0.18 eV for Zntpp(OMe)$_2$−H$_2$pyp$_3$p(OMe), since the oxidation potential in dichloromethane is 0.65 V vs Fc$^+$/Fc for H$_2$pyp$_3$p(Cl), 0.58 V for H$_2$pyp$_3$p, 0.48 V for H$_2$pyp$_3$p(OMe), and 0.30 V for Zntpp(OMe)$_2$. The order of the driving force for the intramolecular electron transfer in the heterodimer agrees with the order of the magnitude of the photocurrent. This suggests that the photocurrent increases as the charge-separated dimer is easily photoproduced in the Schottky barrier.

Figure 6 shows the R dependence of the ϕ value at the Soret peak wavelength for the photocells with Zntpp(OMe)$_2$−H$_2$pyp$_3$p and Zntpp(OMe)$_2$−H$_2$tpp(Cl), where dark-conducting carriers in these mixed solids and the pure porphyrin solids are holes. The thermodynamic driving force for the electron transfer from the Zntpp(OMe)$_2$ in the ground state to the excited metal-free porphyrin is larger in the Zntpp(OMe)$_2$−H$_2$tpp(Cl) (0.32 eV) than in the Zntpp(OMe)$_2$−H$_2$pyp$_3$p (0.28 eV), since the oxidation potential in dichloromethane is 0.62 V vs Fc$^+$/Fc for H$_2$tpp(Cl) and 0.58 V for H$_2$pyp$_3$p. Nevertheless, the photocurrent is larger for the photocell with the latter system than for that with the former system. Though photocurrent maxima are obtained around $R = 0.5$ in both cells, the Soret peak wavelength in the absorption spectra of the Zntpp(OMe)$_2$−H$_2$tpp(Cl) solid films merely shifts to shorter wavelength with increasing R, but the peak wavelength in the absorption spectra of the Zntpp(OMe)$_2$−H$_2$pyp$_3$p solid films exhibits a maximum around $R = 0.5$ because of the axial coordination (see the inset in Figure 6). However, the absorption spectrum of the equimolar Zntpp(OMe)$_2$−H$_2$pyp$_3$p solid film does not show any extra signal indicating a particular interaction between the porphyrin rings. These results suggest that though an electron-donating Zntpp(OMe)$_2$ and an electron-accepting H$_2$tpp(Cl) can exist close to each other by an electrostatic interaction, they cannot exist as closely as both molecules in the Zntpp(OMe)$_2$−H$_2$pyp$_3$p system, being close due to the coordinate bond. Therefore, the photo-

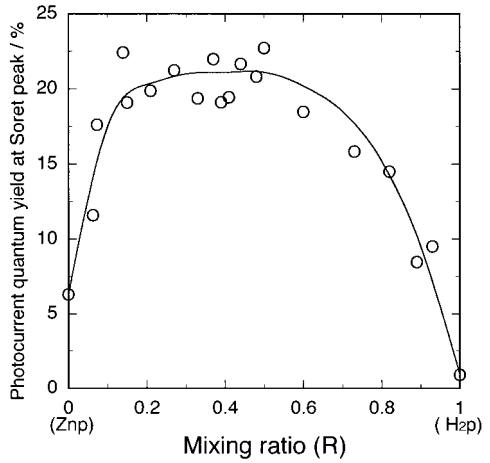

Figure 7. Relation between mixing ratio (R) and short-circuit photocurrent quantum yield at the Soret peak for an Al/Zntpp(OMe)$_2$−H$_2$py$_2$p$_2$p/Au cell. The film thickness of the porphyrin solid is about 20 nm, and the irradiation is done from the Al side by monochromatic light of the Soret peak wavelength with an intensity of about 8 ± 2 μW cm^{-2}.

induced intermolecular electron transfer in the Zntpp(OMe)$_2$−H$_2$tpp(Cl) system is not as easy as the photoinduced intramolecular electron transfer in the Zntpp(OMe)$_2$−H$_2$pyp$_3$p heterodimer. This implies that the ease of the photoproduction of the charge-separated dimer is limited not only by the thermodynamic factor but also by the molecular configuration.

Figure 7 shows the R dependence of the ϕ value at the Soret peak wavelength for the photocell with a mixed solid of Zntpp(OMe)$_2$ and H$_2$py$_2$p$_2$p, where dark-conducting carriers in the mixed solid and the pure porphyrin solids are holes. The enhanced photocurrent is observed over a wide R range in contrast to the R dependence for the mixed systems containing metal-free porphyrins with one pyridyl group as shown in Figure 5. This indicates that because one H$_2$py$_2$p$_2$p molecule has two pyridyl groups in the cis position functioning as a bridging ligand for the formation of a dimer rather than a trimer owing to steric hindrance, the probability of dimerization by the coordination is large even at a mixing ratio other than $R = 0.5$, resulting in the photoproduction of many charge-separated dimers over a wide R range.

The parameters showing the performance of various Al/dye/Au sandwich-type cells with the pure porphyrin solids and the mixed solids are summarized in Table 1. In this work, best values of ϕ =22.5%, $V_{oc} = 0.89$ V, ff = 0.21, and $\eta = 1.50\%$ are obtained for the Al/Zntpp(OMe)$_2$−H$_2$py$_2$p$_2$p ($R = 0.48$, $d = 19$ nm)/Au cell when monochromatic light of $\lambda = 445$ nm with $I_0 = 8$ μW cm^{-2} is illuminated from the Al side.

Discussion

The short-circuit dark currents are hardly detected for the Al/dye Schottky barrier cells with zinc porphyrins, metal-free porphyrins, and porphyrin heterodimers used here. Namely, chemical corrosion of Al by these porphyrins does not occur in the dark, although metal-free tetrabenzporphyrin and metal-free phthalocyanine corrode Al, as we have pointed out in ref 26. This difference is explained by the reason that the oxidation of the porphyrins used here is more difficult than that of the benzporphyrin and the phthalocyanine. Hence, photocorrosion may be also suppressed for porphyrins with high ionization potential as used in this study. However, since the excited dyes are oxidized much more easily than the dyes in the ground state, it is unwarranted that the photocorrosion of Al does not occur

SCHEME 1: Charge-Generation Process from Excited Heterodimer under Large External Electric Field (See Text for the Meaning of Symbols)

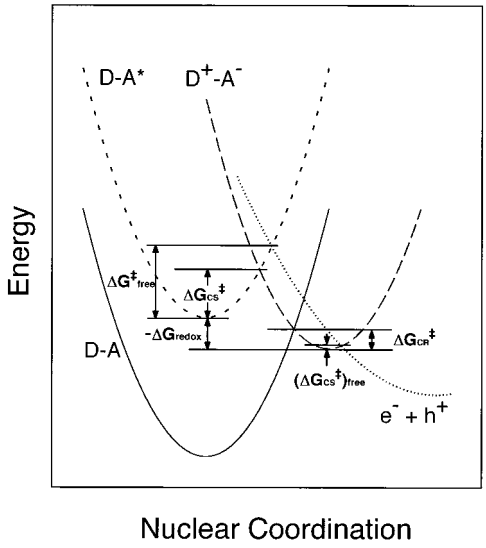

by the porphyrins used here. The photocurrents of the pure porphyrin cells and the mixed porphyrin cells actually decreased to about half after monochromatic light of the Soret peak wavelength with about 8 μW cm^{-2} intensity irradiated the Al/porphyrin interface from the Al side for each cell for 1 h. Whether the photocurrent is from the energy conversion or from the photocorrosion, the rate-determining process for the photocurrent generation is common; that is, it is the dissociation of the excitons in the Al/dye Schottky barrier. In fact, the optical filter effect of the photocurrent observed in this study is reproduced by Yamashita's model[69] assuming that the magnitude of the photocurrent is determined by the ease of charge separation of the excitons diffusing toward the Al/dye interface with an electric field in the depletion layer (see Figure 4). Therefore, the efficiency of charge separation must be improved first for increasing the photocurrent. Then, to take out the final output as the energy-converted photocurrent, the photocorrosion must be avoided. Because our final aim is to obtain high-efficiency solar cells, we will use, for example, the most suitable organic electron acceptor with Au electrode instead of Al electrode for practical use. In this case, a potential gradient for obtaining free charges from excitons may be produced near the organic electron acceptor/porphyrin interface in which photocorrosion does not occur, and the Au electrode makes ohmic contact with the organic electron acceptor. However, such a practical system is complicated for understanding the roles of dyes for charge separation. Therefore, we used Al electrode, which makes the system simple, for screening the good candidates of charge-separation porphyrins. As far as focusing on increasing the efficiency of charge separation, it is no matter whether the subsequent process is energy conversion or photocorrosion.

When a dye solid film is prepared by mixing a weak electron-donating Zntpp(OMe)$_2$ and a weak accepting metal-free porphyrin by means of a spin-coating method that can attain a molecular level mixing, both molecules approach on account of an electrostatic interaction and a coordinate bond. The donating and accepting dyes are represented by D and A, respectively, and the aggregate is denoted by D−A. Because energy transfer from the excited D to the A in the ground state always occurs under illumination, the excited D−A is represented by D−A*, where only A is excited. The D−A* migrates into the built-in potential formed near the Al/porphyrin interface,

and then electrons are transferred from the ground-state D to the excited A, resulting in a charge-separated dimer, D^+-A^-. This is supported from results that the increased fluorescence originating from metal-free porphyrin is observed for the heterodimer solid on glass substrates and that the optical filter effect of the photocurrent observed for the Zntpp$(OMe)_2-H_2$-pyp$_3$p cell is reproduced by Yamashita's model. This photoinduced electron transfer is easier the smaller its activation energy, $\Delta G_{CS}^{\ddagger}$, is. The $\Delta G_{CS}^{\ddagger}$ is limited by both the difference between the redox potentials of the D and A molecules, $-\Delta G_{redox}$, and the configuration between the D and A molecules. If the photoproduced D^+-A^- has arranged favorably for charge generation in the built-in potential, it easily separates into free charges under the electric field,[63,64] although the D^+-A^- rapidly deactivates to the D−A in the ground state by a back-electron-transfer in the absence of an electric field. That is, since the activation energy for obtaining free charges from the D^+-A^-, $(\Delta G_{CS}^{\ddagger})_{free}$, is much smaller than that for the back-electron-transfer ($\Delta G_{CR}^{\ddagger}$) under a large electric field, the D^+-A^- can easily produce a free electron and hole, $e^- + h^+$; namely, enhanced photocurrent is obtained. Further, the free charges are obtained from the D^+-A^- much more easily than from the excited pure D and A molecules because the positive and negative charges are apart from each other in the D^+-A^- compared to those in the excited pure molecules. Eventually, Coulomb's force between the opposite charges is smaller in the former than in the latter. That is, the activation energy for obtaining free charges under the electric field is much smaller for the D^+-A^- than for the excited pure molecules, namely, $(\Delta G_{CS}^{\ddagger})_{free} \ll (\Delta G^{\ddagger})_{free}$.

Even though 0.3 eV of thermodynamic driving force for the photoinduced intramolecular electron transfer in the porphyrin heterodimer exists, the electron transfer does not proceed spontaneously. Only under a built-in potential of about 10^5 V cm^{-1} created near the Al/heterodimer interface is $\Delta G_{CS}^{\ddagger}$ reduced, resulting in the electron transfer. Although $\Delta G_{CS}^{\ddagger}$ is governed by $-\Delta G_{redox}$ and the configuration between D and A, the increase of $-\Delta G_{redox}$ by the built-in potential is small because the magnitude of 10^5 V cm^{-1} is smaller than the already-existing local potential of 10^6 V cm^{-1} in the excited heterodimer, which is estimated from the ratio of thermodynamic driving force (0.3 eV) to the electron-transport distance (less than 1 nm). This means that the role of the built-in potential is for leading the heterodimer to a favorable configuration, bringing out the reduction of $\Delta G_{CS}^{\ddagger}$ and finally intramolecular electron transfer. Because the $(\Delta G_{CS}^{\ddagger})_{free}$ value may be very small and that it may be much smaller than the $\Delta G_{CR}^{\ddagger}$ value, the ease of formation of free charges, namely, the magnitude of the photocurrent, is determined by the ease of the photoproduction of the charge-separated dimer limited by the $\Delta G_{CS}^{\ddagger}$. In fact, for heterodimers with similar configurations, such as Zntpp-$(OMe)_2-H_2$pyp$_3$p(Cl), Zntpp$(OMe)_2-H_2$pyp$_3$p, and Zntpp-$(OMe)_2-H_2$pyp$_3$p(OMe), the photocurrent increases with an increase of $-\Delta G_{redox}$, leading to a decrease of $\Delta G_{CS}^{\ddagger}$. Further, since Zntpp$(OMe)_2-H_2$pyp$_3$p has a closer configuration by the coordination than Zntpp$(OMe)_2-H_2$tpp(Cl), the probability of the photoinduced electron transfer, which forms the charge-separated dimer, is larger for the former system than for the latter system. This results in a larger photocurrent for the former system despite the former $-\Delta G_{redox}$ being smaller than the latter $-\Delta G_{redox}$.

In conclusion, the enhanced photocurrent is obtained for the Al/dye Schottky barrier cell with the porphyrin heterodimer because the photoinduced intramolecular electron transfer occurs easily in the dimer present in the depletion layer of the cell and free charges are easily obtained from the charge-separated dimer.

Acknowledgment. The present research was partly supported by the New Energy and Industrial Technology Development Organization (NEDO).

References and Notes

(1) Merritt, V. Y.; Hovel. H. J. *Appl. Phys. Lett.* **1976**, *29*, 414.
(2) Fan, F.; Faulkner, L. R. *J. Chem. Phys.* **1978**, *69*, 3334.
(3) Ghosh, A. K.; Feng, T. *J. Appl. Phys.* **1978**, *49*, 5982.
(4) Loutfy, R. O.; Sharp, J. H. *J. Chem. Phys.* **1979**, *71*, 1211.
(5) Popovic, Z. D. *Appl. Phys. Lett.* **1979**, *34*, 694.
(6) Loutfy, R. O.; Sharp, J. H.; Hsiao, C. K.; Ho, R. *J. Appl. Phys.* **1981**, *52*, 5218.
(7) Skotheim, T.; Yang, J. M.; Otvos, J.; Klein, M. P. *J. Chem. Phys.* **1982**, *77*, 6144.
(8) Morel, D. L.; Stogry, E. L.; Ghosh, A. K.; Feng, T.; Purwin, P. E.; Shaw, R. F.; Fishman, C. *J. Phys. Chem.* **1984**, *88*, 923.
(9) Kampas, F. J.; Yamashita, K.; Fajar, J. *Nature* **1980**, *284*, 40.
(10) Yamashita, K.; Kihara, N.; Shimidzu, H.; Suzuki, H. *Photochem. Photobiol.* **1982**, *35*, 1.
(11) Yamashita, K.; Harima, Y.; Matsubayashi, T. *J. Phys. Chem.* **1989**, *93*, 5311.
(12) Harima, Y.; Miyatake, M.; Yamashita, K. *Chem. Phys. Lett.* **1992**, *200*, 263.
(13) Harima, Y.; Takeda, K.; Yamashita, K. *J. Phys. Chem. Solids* **1995**, *56*, 1223.
(14) Kearns, D. R.; Tollin, G.; Calvin, M. *J. Chem. Phys.* **1960**, *32*, 1020.
(15) Loutfy, R. O.; Menzel, E. R. *J. Am. Chem. Soc.* **1980**, *102*, 4967.
(16) Chamberlain, G. A. *J. Appl. Phys.* **1982**, *53*, 6262.
(17) Harima, Y.; Yamamoto, K.; Takeda, K.; Yamashita, K. *Bull. Chem. Soc. Jpn.* **1989**, *62*, 1458.
(18) Takahashi, K.; Horino, K.; Komura, T.; Murata, K. *Bull. Chem. Soc. Jpn.* **1993**, *66*, 733.
(19) Tang, C. W. *Appl. Phys. Lett.* **1986**, *48*, 183.
(20) Shichiri, T.; Suezaki, M.; Inoue, T. *Chem. Lett.* **1992**, 1717.
(21) Hiramoto, M.; Fukusumi, H.; Yokoyama, M. *Appl. Phys. Lett.* **1992**, *61*, 2580.
(22) Hiramoto, M.; Fujiwara, H.; Yokoyama, M. *J. Appl. Phys.* **1992**, *72*, 3781.
(23) Takahashi, K.; Nakatani, S.; Matsuda, T.; Nanbu, H.; Komura, T.; Murata, K. *Chem. Lett.* **1994**, 2001.
(24) Murata, K.; Ito, S.; Takahashi, K.; Hoffman, B. M. *Appl. Phys. Lett.* **1996**, *68*, 427.
(25) Takahashi, K.; Nakatani, S.; Yamaguchi, T.; Komura, T.; Ito, S.; Murata, K. *Sol. Energy Mater. Sol. Cells* **1997**, *45*, 127.
(26) Murata, K.; Ito, S.; Takahashi, K.; Hoffman, B. M. *Appl. Phys. Lett.* **1997**, *71*, 674.
(27) Fujihira, M.; Sakomura, M.; Kamei, T. *Thin Solid Films* **1989**, *180*, 43.
(28) Akiyama, K.; Nishikawa, S.; Ueyama, S.; Isoda, S. *Jpn. J. Appl. Phys.* **1995**, *34*, 3942.
(29) Hosono, H.; Kaneko, M. *J. Chem. Soc., Faraday Trans*. **1997**, *93*, 1313.
(30) Akiyama, T.; Imahori, H.; Ajawakom, A.; Sakata, Y. *Chem. Lett.* **1996**, 907.
(31) Kondo, T.; Yanagida, M.; Nomura, S.; Ito, T.; Uosaki, K. *J. Electroanal. Chem.* **1997**, *438*, 121.
(32) Uosaki, K.; Kondo, T.; Zhang, X. Q.; Yanagida, M. *J. Am. Chem. Soc.* **1997**, *119*, 8367.
(33) Diarra, A.; Hotchandani, S.; Max, J.-J.; Leblanc, R. M. *J. Chem. Soc., Faraday Trans. 2* **1986**, *82*, 2217.
(34) Desormeaux, A.; Max, J. J.; Leblanc, R. M. *J. Phys. Chem.* **1993**, *97*, 6670.
(35) Takahashi, K.; Nanbu, H.; Komura, T.; Murata, K. *Chem. Lett.* **1993**, 613.
(36) Takahashi, K.; Hashimoto, K.; Komura, T.; Murata, K. *Chem. Lett.* **1994**, 269.
(37) Takahashi, K.; Nakamura, J.; Yamaguchi, T.; Komura, T.; Ito, S.; Murata, K. *J. Phys. Chem. B* **1997**, *101*, 991.
(38) Takahashi, K.; Higashi, M.; Tsuda, Y.; Yamaguchi, T.; Komura, T.; Ito, S.; Murata, K. *Thin Solid Films* **1998**, *333*, 256.
(39) Takahashi, K.; Etoh, K.; Tsuda, Y.; Yamaguchi, T.; Komura, T.; Ito, S.; Murata, K. *J. Electroanal. Chem.* **1997**, *426*, 85.
(40) Uehara, K.; Ichikawa, T.; Matsumoto, K.; Sugimoto, A.; Tsunooka, M.; Inoue, H. *J. Electroanal. Chem.* **1997**, *438*, 85.
(41) Yu, G.; Heeger, A. J. *J. Appl. Phys.* **1995**, *78*, 4510.
(42) Sariciftci, N. S.; Smilowitz, L.; Heeger, A. J.; Wuld, F. *Science* **1992**, *258*, 1474.

(43) Roman, L. S.; Andersson, M. R.; Yohannes, T.; Inganas, O. *Adv. Mater*. **1997**, *9*, 1164.
(44) Wang, Y.; Suna, A. *J. Phys. Chem. B* **1997**, *101*, 5627.
(45) Tabushi, I.; Koga, N.; Yanagita, M. *Tetrahedoron Lett.* **1979**, 257.
(46) Kong, J. L. Y.; Spears, K. G.; Loach, P. A. *Photochem. Photobiol.* **1982**, *35*, 545.
(47) Harrimann, A.; Porter, G.; Wilowska, A. *J. Chem. Soc., Faraday Trans. 2* **1984**, *80*, 191.
(48) Gubelmann, M.; Harriman, A.; Lehn, J. M.; Sessler, J. L. *J. Phys. Chem.* **1990**, *94*, 308.
(49) Nakamura, H.; Motonaga, A.; Ogata, T.; Nakao, S.; Nagamura, T.: Matsuo, T. *Chem. Lett.* **1986**, 1615.
(50) Saito, T.; Hirata, Y.; Sato, H.; Yoshida, T.; Mataga, N. *Bull. Chem. Soc. Jpn.* **1988**, *61*, 1925.
(51) Takahashi, K.; Terashima, T.; Komura, T.; Imanaga, H. *Bull. Chem. Soc, Jpn.* **1989**, *62*, 3069.
(52) Takahashi, K.; Hase, S.; Komura, T.; Ohno, O. *Bull. Chem. Soc. Jpn.* **1992**, *65*, 1475.
(53) Nishitani, S.; Kurata, N.; Sakata, Y.; Misumi, S.; Karen, A.; Okada, T.; Mataga, N. *J. Am. Chem. Soc.* **1983**, *105*, 7771.
(54) Leland, B. A.; Joram, A. D.; Felder, P. M.; Hopfield, J. J.; Zewail, A. H.; Dervan, P. B. *J. Phys. Chem.* **1985**, *89*, 5571.
(55) Wasielewski, M. R.; Niemczyk, M. P.; Svec, W. A.; Pewitt, E. B. *J. Am. Chem. Soc.* **1985**, *107*, 5562.
(56) Schmidt, J. A.; McIntosh, A. R.; Weedon, A. C.; Bolton, J. R.; Connolly, J. C.; Hurley, J. K.; Wasielewski, M. R. *J. Am. Chem. Soc.* **1988**, *110*, 1733.
(57) Gust, D.; Moore, T. A.; Moore, A. L.; Makings, L. R.; Seely, G. R.; Ma, X.; Trier, T. T.; Gao, F. *J. Am. Chem. Soc.* **1988**, *110*, 7567.
(58) Osuka, A.; Nakajima, S.; Okada, T.; Taniguchi, K.; Nozaki, K.; Ohno, T.; Yamazaki, I.; Nishimura, Y.; Mataga, N. *Angew. Chem., Int. Ed. Engl.* **1996**, *35*, 92.
(59) Osuka, A.; Mataga, N.; Okada, T. *Pure Appl. Chem.* **1997**, *69*, 797.
(60) Collin, J. P.; Harriman, A.; Heitz, V.; Odobel, F.; Sauvage, J. P. *Coord. Chem. Rev.* **1996**, *148*, 63.
(61) Sakata, Y.; Imahori, H.; Tsue, H.; Higashida, S.; Akiyama, T.; Yoshizawa, E.; Aoki, M.; Yamada, K.; Hagiwara, K.; Taniguchi, S.; Okada, T. *Pure Appl. Chem.* **1997**, *69*, 1951.
(62) Imahori, H.; Sakata, Y. *Adv. Mater*. **1997**, *9*, 537.
(63) Galoppini, E.; Fox, M. A. *J. Am. Chem. Soc.* **1996**, *118*, 2299.
(64) Fox, M. A.; Galoppini, E. *J. Am. Chem. Soc.* **1997**, *119*, 5277.
(65) Fleischer, E. B.; Shachter, A. M. *Inorg. Chem.* **1991**, *30*, 3763.
(66) Alder, A. D.; Longo, R. F.; Finarelli, J. D.; Assour, J.; Korsakoff, L. *J. Org. Chem.* **1967**, *32*, 476.
(67) Alder, A. D.; Longo, R. F.; Kampas, F.; Kim, L. *J. Inorg. Nucl. Chem.* **1970**, *32*, 2443.
(68) Nappa, M.; Valentine, J. S. *J. Am. Chem. Soc.* **1978**, *100*, 5075.
(69) Yamashita, K.; Harima, Y.; Iwashima, H. *J. Phys. Chem.* **1987**, *91*, 3055.